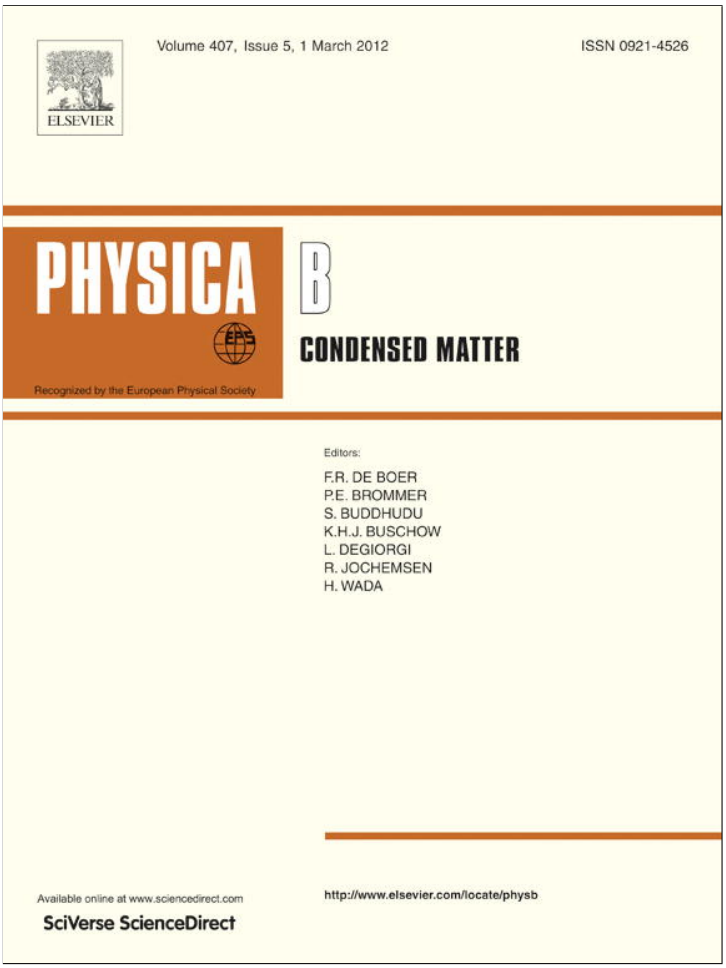

Physica B 407 (2012) 855–858

Contents lists available at SciVerse ScienceDirect

Physica B

journal homepage: www.elsevier.com/locate/physb

Graphene based single molecule nanojunction

R. Chowdhury *, S. Adhikari, P. Rees

Multidisciplinary Nanotechnology Centre, Swansea University, Swansea SA2 8PP, UK

ARTICLE INFO

Article history:
Received 24 August 2011
Received in revised form
13 December 2011
Accepted 15 December 2011
Available online 22 December 2011

Keywords:
Graphene fragment
Ab-initio
Single-electron transistor
Coulomb blockade

ABSTRACT

We introduce the ab-initio framework for zigzag-edged graphene fragment based single-electron transistor (SET) operating in the Coulomb blockade regime. Graphene is modeled using the density-functional theory and the environment is described by a continuum model. The interaction between graphene and the SET environment is treated self-consistently through the Poisson equation. We calculate the charging energy as a function of an external gate potential, and from this we obtain the charge stability diagram. Specifically, the importance of including re-normalization of the charge states due to the polarization of the environment has been demonstrated.

1. Introduction

Recent developments in semiconductor theory have led to the new field of device research focusing on structures capable of exploiting the discreteness of the electron charge [1–3]. Their operation is based on the discrete nature of electrons tunneling through thin potential barriers. These devices are commonly referred to as single-electron transistor (SET) [4,5]. It consists of a gate electrode that electrostatically influences electrons traveling between the source and drain electrodes. The electrons in SET need to cross two tunnel junctions that form an isolated conducting electrode called the island. It allows to control current consisting of electrons traversing the device one by one, by varying the charge on the control gate by a fraction of an electron [6]. While SETs are extremely and exceedingly sensible to the presence of single charged defects, impressive reproducibility has been recently obtained through refined fabrication techniques [7–9].

Graphene has been recognized as a new revolutionary material for electronics. Compared to silicon and GaAs based classical semiconducting materials, the understanding of electronic transport in graphene [10] is still in its infancy. Confinement effects typically of mesoscopic systems and electron–electron interactions [11,12] are expected to play a crucial role on the transport properties [13,14] in graphene [15]. Recently a tunable SET has been demonstrated in a graphene island weakly coupled to leads [16]. Theoretical investigations [17,18] have attributed the existence of such a gap to Coulomb interaction effects [19]. Nonequilibrium Greens functions (NEGF) within with density-functional theory (DFT) [20] or semiempirical models [21] have been successfully used in modeling coherent transport for various types of molecular junctions. However, in the case of molecular SET [22], the transport is incoherent [23]. Although there are very limited recently published experimental results [19] on the characterization of graphene-based SET, theoretical studies [11,24] are not widely reported. Theoretical studies [25] can enhance the understanding of these novel devices and contribute towards future designs. Motivated by this, in this article we introduced the ab-initio framework of SET's operating in the Coulomb blockade regime [26]. We use the model to calculate the charging energy of graphene with zigzag edge in an electrostatic environment [25] resembling a SET geometry. We calculate the charging energy as a function of an external gate potential, and from this we obtain the charge stability diagram. Specifically, the importance of including re-normalization [27] of the molecular charge states due to the polarization of the environment has been demonstrated.

2. Modelling and simulation

The calculation uses DFT based NEGF formalism within TransSIESTA [28–31] framework, which is implemented in Atomistix ToolKit [32]. The DFT model used here is based on pseudopotentials with numerical localized basis functions. In this framework, a compensation charge $\rho_i^{comp}(\mathbf{r})$ is introduced for each atomic site. The compensation charge has the same charge Z_i as the pseudopotential, and is used to screen the electrostatic interactions. Next, we extend the total energy functional to include interactions with a number of dielectric and metallic regions surrounding the system. Fig. 1 illustrates a typical SET geometry, where

* Corresponding author. Tel.: +44 1792 602969; fax: +44 1792 295676.
E-mail address: R.Chowdhury@swansea.ac.uk (R. Chowdhury).

0921-4526/$ - see front matter © 2011 Elsevier B.V. All rights reserved.
doi:10.1016/j.physb.2011.12.101

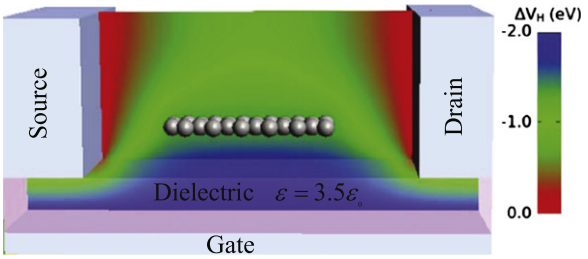

Fig. 1. Graphene fragment with zigzag edge (width=7.104 Å and length=13.554 Å) in the SET environment considered in this paper. The electrostatic environment model includes graphene on top of 3.7 Å thick dielectric substrate with a metallic back-gate, and surrounded by source and drain gold electrodes (W=5.28 eV) with source–drain distance of about 27 Å. The contour plot shows the induced electrostatic potential for a gate voltage of 2 V and zero source–drain bias.

graphene fragment with zigzag edge (width=7.104 Å and length=13.554 Å) is positioned on top of a dielectric material and surrounded by metallic electrodes.

Within the metallic regions the potential is fixed to the applied voltage on each respective electrode, and on the faces of the cell we apply Neumann boundary conditions, i.e., zero electric field. The system consists of a metallic back-gate, and above the gate there is 6.7 Å of dielectric material with dielectric constant $3.5\varepsilon_0$. Graphene is positioned 1.2 Å above the dielectric. To the left and right of the graphene are metallic source–drain electrodes, and the distance between graphene and the electrodes is 6.5 Å. We note that for a typical metal surface the image plane is 2.0 Å above the surface, and to compare with atomic adsorption geometries, this length must be added to the above distances. To obtain the energies, we first calculate the charging energies of the isolated zigzag graphene. We obtain the charging energy by performing self-consistent calculations for the N and $N+1$ charge states of the isolated zigzag graphene and subtracting their total energies. For the calculation we use DFT in the spin polarized local density approximation [33] and expand the wavefunctions in a double-ζ polarized basis set. The geometries are obtained by relaxing the graphene fragment with zigzag edge in the neutral state. Following are program parameters used in the present analyses: (i) basis set parameters: Type=double-ζ polarized; (ii) exchange correlation parameter: type=LDA, functional=PZ; (iii) density mesh cut-off=75 Hartree, k-point sampling=$15\times15\times15$, Electron temperature=300 K; (iv) Iteration control parameters: tolerance=10^{-5}, algorithm=PaulayMixer, mixing variable=Hamiltonian variables.

3. Results and discussion

To validate the modelling and methodology adopted, we start our calculation with benzene. The charging energies of the isolated benzene and benzene in SET environment are calculated. We obtain $E_I-E_A=11.48$ eV and $E_I-E_A=7.68$ eV, in the isolated phase and SET environment, respectively. Excellent agreement has been obtained compared with the available results [23]. Being confident about the agreement of the charging energies estimation, analysis of the graphene with zigzag edge is considered next.

The ionization energy (E_I) and the affinity energy (E_A) of the graphene (with electrode-to-graphene distantace=6.5 Å) are obtained as 6.58 eV and 3.71 eV in isolated phase. Similarly, E_I and E_A of the graphene is obtained as 5.97 eV and 4.24 eV in SET environment. Table 1 shows the calculated charging energies of the system for different configurations. We calculate the total energy of the different charge states of the SET system as a function of the gate potential. The results are shown in Fig. 2. The total energy includes the reservoir energy qW, where q being the charge of graphene and W (=5.28 eV) is the work function of the gold electrode. Fig. 2 shows that the neutral graphene has the lowest energy at zero gate potential. The state with the lowest energy is the stable charge state of the graphene for a given gate voltage. Negative gate voltages stabilize positive ions, while positive gate voltages stabilize negative ions. In the region around zero gate voltage, the neutral state is the lowest energy state. At negative gate potentials the positive charge states are stabilized, while the negative charge states are stabilized at positive gate potentials. This is in agreement with HOMO and LUMO levels following $-eV_G$; thus, at positive bias the LUMO level gets below the electrode Fermi level and attracts an electron, and graphene becomes negatively charged. At negative gate potentials the HOMO level gets above the electrode Fermi level and an electron is escaping from graphene, which becomes positively charged. The gate dependence is close to linear, and the slope is related to the charge state of graphene. To understand the dependence between the total energy and the gate potential, we fit a quadratic function to the data:

$$E=\alpha qV_G+\beta(eV_G)^2 \quad (1)$$

Note that we assume the linear term to be proportional to the charge q on graphene, while the quadratic term arises from the polarization of the graphene and therefore is independent of q. By fitting the data in Fig. 2(a), we find for graphene $\alpha=0.7043$, $\beta=-0.003$ eV^{-1}, where the variation with the charge state is ~0.01 for α and ~0.001 eV^{-1} for β. Thus, graphene is strongly coupled with the gate. Similarly, by fitting the data in Fig. 2(c), we find for graphene $\alpha=0.644$, $\beta=-0.003$ eV^{-1} and by fitting the data in Fig. 2(e), we find for graphene $\alpha=0.456$.

This is due to the fact that the carbon atoms in graphene on average are closer to the dielectric substrate. Therefore, graphene shows an almost linear relationship between the total energy and the gate potential, since all atoms are almost identically shifted by the gate potential. This is illustrated by the induced potential of the graphene SET shown in Fig. 1. From the contour plot we see that the potential is almost constant at the carbon atoms and has a value ~-1.2 eV. Dividing with the gate potential -2 eV, we estimate $\alpha\sim0.6$ in good agreement with the quadratic fit above. We can estimate the charge stability diagram from the total energies, which is shown in Fig. 2(b), (d) and (e) for electrode to graphene distance=5 Å, 6.5 Å and 10 Å, respectively. Different colors presents different number of charge states within the bias window. For the system considered, the excitation energy of the second electron is much smaller than for the first electron. It can also be noted that, in the charge stability diagram the nonlinear dependence of the total energy on the gate potential is not observed. This is due to fact that, the charge stability diagram depends only on the differences in energies between the charge states, and the second-order term in Eq. (1) is independent of the charge state.

Table 1
Ionization (I) and affinity (A) energies for different configurations of the system. The distance is measured from electrode to graphene. The distances are varied from 5 Å to 13 Å.

Distance (Å)	E_I^{+1} (eV)	E_I (eV)	E_A (eV)	E_A^{-1} (eV)
5.0	7.76	5.98	−4.22	−2.46
6.5	7.70	5.97	−4.24	−2.51
10.0	7.40	5.89	−4.36	−2.87
13.0	5.99	5.49	−4.99	−4.54

4. Conclusion

In conclusion, we exploited the use of the graphene fragment with zigzag edge for single-electron transistor. Ab-initio framework

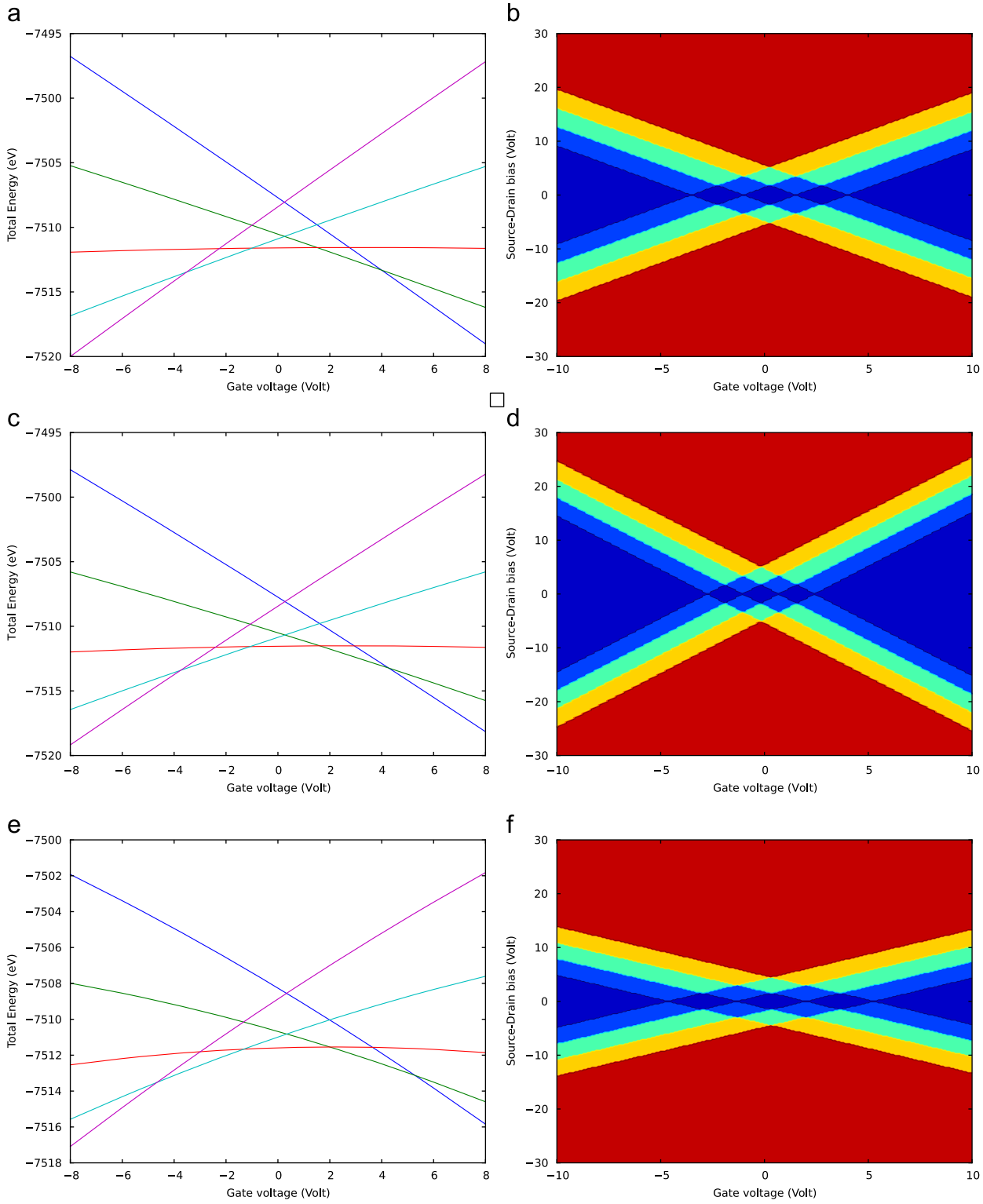

Fig. 2. (a), (c), (e) The total energy as function of the gate voltage for graphene in the SET environment. Different curves are for different charge states of graphene, blue (−2), green (−1), red (0), turquoise (1), and violet (2); (b), (d), (f) The charge stability diagram for graphene within the SET environment at the zero gate voltage. It is assumed that there is a linear relation between the charging energy and the gate voltage. The colors show the number of charge states in the bias window for a given gate voltage. The color map is blue (−2), light blue (−1), red (0), green (1), and orange (2). (a) Variation of total energy with gate voltage: elec-trode to graphene distance=5Å; (b) Charge stability diagram: electrode to graphene distance=5Å; (c) Variation of total energy with gate voltage: elec-trode to graphene distance=6.5Å; (d) Charge stability diagram: electrode to graphene distance=6.5Å; (e) Variation of total energy with gate voltage: elec-trode to graphene distance=10Å and (f) Charge stability diagram: electrode to graphene distance=10Å. (For interpretation of the references to color in this figure legend, the reader is referred to the web version of this article.)

has been employed for calculating the charging energy of graphene in a metallic environment. We calculated the charging energy as a function of the gate potential. The present study further demonstrates the use of first-principles to gain new insight into the properties of single-electron transistors operating in the Coulomb blockade regime. Importance of including re-normalization

of the molecular charge states due to the polarization of the environment has been demonstrated. It is expected that chemical/edge modifications and/or altering geometric configuration, effect of source–drain distance, may tune graphene-based single electron transistor, which is focused as a follow-up work, to widen the applications of this novel material.

References

[1] D. Darau, G. Begemann, A. Donarini, M. Grifoni, Phys. Rev. B 79 (23) (2009) 235404.
[2] K. Moth-Poulsen, T. Bjornholm, Nat. Nanotechnol. 4 (9) (2009) 551.
[3] G. Fiori, M. Pala, G. Iannaccone, IEEE Trans. Nanotechnol. 4 (4) (2005) 415.
[4] C.R. Wolf, K. Thonke, R. Sauer, Appl. Phys. Lett. 96 (14) (2009) 142108.
[5] S. Andergassen, V. Meden, J. Splettstoesser, H. Schoeller, M.R. Wegewijs, Nanotechnology 21 (27) (2010) 272001.
[6] K. Likharev, Proc. IEEE 87 (4) (1999) 606.
[7] K. Nishiguchi, H. Inokawa, Y. Ono, A. Fujiwara, Y. Takahashi, IEEE Electron Device Lett. 25 (1) (2004) 31.
[8] S.I. Khondaker, K. Luo, Z. Yao, Nanotechnology 21 (9) (2010) 095204.
[9] A. Fujiwara, Y. Takahashi, K. Yamazaki, H. Namatsu, M. Nagase, K. Kurihara, K. Murase, IEEE Trans. Electron Devices 46 (5) (1999) 954.
[10] A. Danilov, S. Kubatkin, S. Kafanov, P. Hedegard, N. Stuhr-Hansen, K. Moth-Poulsen, T. Bjornholm, Nano Lett. 8 (1) (2008) 1.
[11] S. Koller, L. Mayrhofer, M. Grifoni, Europhys. Lett. 88 (5) (2009) 57001.
[12] F. Withers, M. Dubois, A.K. Savchenko, Phys. Rev. B 82 (7) (2010) 073403.
[13] R. Chowdhury, S. Adhikari, P. Rees, S.P. Wilks, F. Scarpa, Phys. Rev. B 83 (4) (2011) 045401.
[14] S.Z. Bisri, T. Takenobu, T. Takahashi, Y. Iwasa, Appl. Phys. Lett. 96 (18) (2010) 183304.
[15] S.S. Gupta, R.C. Batra, J. Comput. Theor. Nanosci. 7 (10) (2010) 2151.
[16] C. Stampfer, E. Schurtenberger, F. Molitor, J. Guettinger, T. Ihn, K. Ensslin, Nano Lett. 8 (8) (2008) 2378.
[17] F. Sols, F. Guinea, A.H.C. Neto, Phys. Rev. Lett. 99 (16) (2011) 073405.
[18] M. Zarea, N. Sandler, Phys. Rev. Lett. 99 (25) (2007) 256804.
[19] T. Ihn, J. Guettinger, F. Molitor, S. Schnez, E. Schurtenberger, A. Jacobsen, S. Hellmueller, T. Frey, S. Droescher, C. Stampfer, K. Ensslin, Mater. Today 13 (3) (2010) 44.
[20] K. Stokbro, D.E. Petersen, S. Smidstrup, A. Blom, M. Ipsen, K. Kaasbjerg, Phys. Rev. B 82 (7) (2010) 075420.
[21] K. Kaasbjerg, K. Flensberg, Nano Lett. 8 (11) (2008) 3809.
[22] S. Kubatkin, A. Danilov, M. Hjort, J. Cornil, J. Bredas, N. Stuhr-Hansen, P. Hedegard, T. Bjornholm, Nature 425 (6959) (2003) 698.
[23] K. Stokbro, J. Phys. Chem. C 114 (48) (2010) 20461.
[24] Z.-Q. Fan, K.-Q. Chen, Physica E–Low-Dimensional Syst. Nanostruct. 42 (5) (2010) 1492.
[25] E.A. Osorio, K. Moth-Poulsen, H.S.J. van der Zant, J. Paaske, P. Hedegard, K. Flensberg, J. Bendix, T. Bjornholm, Nano Lett. 10 (1) (2010) 105.
[26] R. Stadler, V. Geskin, J. Cornil, Phys. Rev. B 79 (11) (2009) 113408.
[27] K.S. Thygesen, A. Rubio, Phys. Rev. Lett. 102 (4) (2009) 046802.
[28] N.D. Lang, Phys. Rev. B 52 (7) (1995) 5335.
[29] Y. Xue, S. Datta, M. Ratner, Chem. Phys. 281 (2–3) (2002) 151. (Sp. Iss. Sl).
[30] M. Brandbyge, J. Mozos, P. Ordejon, J. Taylor, K. Stokbro, Phys. Rev. B 65 (16) (2002) 165401.
[31] J. Soler, E. Artacho, J. Gale, A. Garcia, J. Junquera, P. Ordejon, D. Sanchez-Portal, J. Phys.: Condens. Matter 14 (11) (2002) 2745.
[32] Atomistix ToolKit (version 11.2), Quantumwise A/S, 2011 〈www.quantumwise.com〉.
[33] U. Treske, F. Ortmann, B. Oetzel, K. Hannewald, F. Bechstedt, Phys. Status Solidi A – Appl. Mater. Sci. 207 (2) (2010) 304.